

Temporal regionalisation of unharmonised data using networks

August 10, 2019

Abstract

This paper proposes a novel method for data-driven identification of spatio-temporal neighbourhoods and their dynamics. Using a simple network representation, the method enables temporal regionalisation *without the need for geographical harmonisation*. The proposed method therefore sidesteps an error-prone process that is nevertheless currently used in virtually all longitudinal analysis of region-based data.

To allow for a transparent corroboration of our method, we use it as a basis for an interactive and intuitive interface for the progressive exploration of the results. The interface gives direct access to the original data to both experts and non-experts, allowing users to characterize broad patterns of stability and change and identify detailed local processes.

We validate our method with illustrative scenarios from Chicago and Toronto, with results that match the established literature. The system is publicly available, with demographic data for over forty regions in the USA and Canada between 1970 and 2010, but the methodology is suitable for any region-based data.

1 Introduction

Neighbourhoods have increasingly become a central concept in social research and targets for social policy (Sampson, 2012; Galster, 2019; Stone et al., 2015; Looker, 2015). To be sure, a focus on neighbourhoods extends to the formative period of the modern social sciences (Abbott, 1997). Recent interest has at least partly been rekindled through newly available longitudinal demographic datasets (Logan et al., 2014; Manson et al., 2017), convenient computational tools (Rey et al., 2018), and new sources of data (Poorthuis, 2018).

25 In this work, we consider neighbourhoods as *formal regions* (Montello, 2003), geographically con-
 26 tinuous areas with similar data characteristics. These advances have made neighbourhood constructs
 27 more tractable to quantitative analysis. Yet new challenges have also emerged, especially at the con-
 28 vergence of research on neighbourhood effects and neighbourhood dynamics. Neighbourhood effects
 29 research assumes knowledge about the nature and scope of "the neighbourhood" that presumably
 30 shapes individual outcomes (Kwan, 2018; Shelton and Poorthuis, 2019). Concurrently, researchers
 31 note that neighbourhoods are not necessarily fixed containers in which other processes occur, but
 32 themselves dynamically evolve (Delmelle, 2017; Reades et al., 2019; Li and Xie, 2018). The result is
 33 to open up key assumptions about neighbourhoods for theoretical and empirical examination: how
 34 do we appropriately define and compare neighbourhoods at a given time?; how do we appropriately
 35 define and compare the temporal trajectories of neighbourhoods?; and can we do both at once, "fully
 36 interactionally" (Abbott, 1997): classify neighbourhoods now based on where they came from and
 37 where they are going?

38 In principle, much of the recent research is committed to the proposition that neighbourhoods
 39 are open and evolving entities. Ironically, its empirical practice tends to rely on methods that require
 40 fixed geographical regions. This requirement is difficult to satisfy, as most longitudinal datasets are
 41 based on pre-defined tabulation areas that are routinely modified by data collection agencies, usually
 42 to follow population changes.

43 The standard approach then is to *geographically harmonise* data. This involves interpolating
 44 existing measurements into a common set of regions (Logan et al., 2014; Hallisey et al., 2017;
 45 Allen and Taylor, 2018). Recent computational tools have somewhat simplified this process (Rey
 46 et al., 2018), but it still involves non-trivial questions: which geometry to use as target, how to
 47 apportion the variables, or how to combine data from different sources. Further, these question
 48 do not necessarily have optimal answers. Indeed, regardless of how well this process is performed,
 49 it still introduces errors (Logan et al., 2016), even when additional data is provided (Eicher and
 50 Brewer, 2001). Essentially, harmonisation generates artificial data points that can potentially lead
 51 to inaccurate results, even though they are seldom interpreted as such. Nevertheless, because there
 52 has been no viable alternative, and the results often appear plausible, these concerns are generally
 53 overlooked. The result is that the harmonisation approach is virtually mandatory in the current
 54 literature: "(...) tract-by-tract comparison is not possible unless data from 2000 is interpolated to
 55 2010 boundaries (...)" (Dmowska et al., 2017), "(...) This limits cross-year comparison since data

are not representative of the same spatial units. (...)” (Allen and Taylor, 2018).

The main contribution of this paper is a method for longitudinal data processing that works with the original data by leveraging a network based representation. It enables tract-by-tract comparison and the identification of patterns of demographic evolution *without geographic harmonisation*.

To allow a proper examination of our method and its results, we built an online interactive system using this representation. It enables users to visualise, interpret, and explore trajectories of neighbourhood change. This interface helps validate our method, by allowing it to be compared to existing and future methods. Further, it is a significant contribution to the research community: it provides a vehicle for quickly and easily grasping complex long-term changes, experimenting with different parameters to interactively learn from data, and making neighbourhood change research publicly transparent. The interface thus responds to increasing concerns about reproducibility and transparency, as well as ongoing attention to the value of visualisation in scientific research and communication.

We start by presenting an intuitive example of our representation in Section 1, then we review the relevant literature on longitudinal studies, data representation, clustering, and spatio-temporal visualisation in Section 3. Our methodology is introduced in detail in Section 4, along with the included interface. Illustrative scenarios for Chicago, Toronto, and Los Angeles are presented in Section 5 and the feedback of five field experts are summarised in Section 6. Our prototype system is available at [\[link\]](#), including more than forty regions in the US and Canada. The source code is publicly available at [\[link\]](#).¹

2 Intuition

While utterly simple, the network model breaks from the deeply rooted traditional tabular paradigm in a significant way. The traditional method requires the data to be treated as a collection of fixed entities with properties that evolve over time – rows in a table with temporal values as columns. By contrast, our method represents each measurement as a separate entity and encodes the evolution of these entities over time.

To ease the cognitive transition to a new paradigm, we start with an intuitive example of how the method works, using a small portion of a fictitious urban region illustrated on the left part of

¹The editors are considering, at our request, an exception to the double-blind requirement to allow access to the system. We provided them with the URLs of the system, code, and documentation separately.

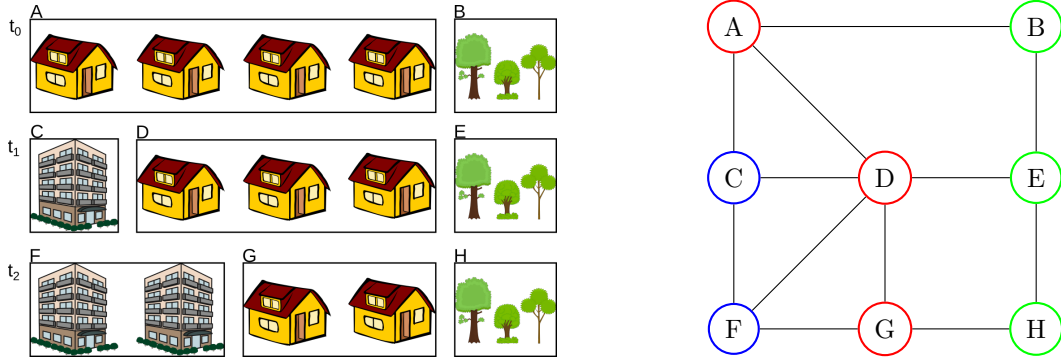


Figure 1: Network based spatio-temporal data representation. **Left:** Three temporal stages of the evolution of a fictitious urban area, with aggregation areas A to H. **Right:** Network representation of the aggregation areas where the colours identify similar regions.

Figure 1. This example includes three different times (t_0, t_1, t_2), with different aggregation areas identified as letters from A to H. For t_0 , the initial time, we have areas A and B, with small houses and a park, respectively. The park remains stable (B, E, and H), but the houses are partially replaced by larger buildings (C and F).

This example illustrates some of the challenges of harmonisation. None of these aggregation areas is clearly suitable as an interpolation target. In fact, adopting any of these areas as a target would require merging heterogeneous regions and/or dividing homogeneous regions. For instance, by choosing the regions of t_1 , A would be split to match regions C and D, which appears to be a rather reasonable approximation in this homogeneous artificial example (even if it commits the fallacy of division). Region F would be similarly split to match C, but F would be split and merged with G to match D, potentially leading to statistical measurements that do not properly represent either region.

Real world measurements are seldom as homogeneous and noise-free as this artificial example. By splitting and merging the data to fit arbitrary borders, that were not necessarily coherent at the time of the measurement, harmonisation increases the distance between measurement and reality.

Instead, we propose a network-based representation. A *network* (also called a *graph*) is a collection of entities (nodes) that are related to each other (edges). In this case, each different aggregation area is represented as a node and we connect nodes that have overlapping geographical areas in different times or are neighbours in the same time, leading to the network illustrated on the right of Figure 1. By partitioning the network into connected nodes that are similar, we are effectively iden-

tifying clusters in the spatio-temporal data, as illustrated by the colours of the nodes on the right side of Figure 1. Further, all the possible paths of change can be obtained by computing sequences of nodes over time, in this case: (A, C, F), (A, D, F), (A, D, G), and (B, E, H). This representation is also suited for geographically consistent regions, as illustrated by the stable park in this example, and is therefore a generalisation of the traditional paradigm.

Note that the edges of this network merely encode that two regions are related. This is binary information, there is no apportionment, no areal measurements, no population percentages associated with the edge. Indeed, our method also connects regions of the same time that share borders, representing exactly that they are neighbouring areas.

In the following, we argue that this network representation allows us to study neighbourhood change in a way that does not require an prior interpolation.

3 Related Work

Since our problem encompasses several fields, we divide this section into specific sub problems: *longitudinal demographic studies*, describing the traditional tabular approach to longitudinal studies; *data representation*, elaborating how evolving geographic data can be represented for processing; *data clustering*, briefly reviewing existing clustering methods; and *cluster characterisation*, articulating how clusters can be visually summarised.

3.1 Longitudinal demographic studies

Census data is used not only to discover demographic patterns (Firebaugh and Farrell, 2016), but to correlate demographic characteristics to other measurements (Diez-Roux et al., 1997). However, longitudinal studies are rare, because they are difficult : ”(...) *One of the most challenging and fascinating areas in spatial statistics is the synthesis of spatial data collected at different spatial scales(...)*” (Gotway and Young, 2002). While census tract level data is readily available for the US since at least 1910 (Manson et al., 2017), most studies consider the period between 1970 and 2010, using pre-harmonised data from the Longitudinal Tract Data Base (Logan et al., 2014). Despite its inherent errors (Logan et al., 2016; Hallisey et al., 2017), this dataset has become [widely adopted, along with the Neighborhood Change Database GeoLytics et al. \(2010\)](#), as source for longitudinal demographic data at the neighbourhood scale, with similar efforts appearing in other

132 countries (Liu et al., 2015; Lee and Rinner, 2015; Allen and Taylor, 2018). These datasets have been
133 highly significant for the field. Yet they also limit the universe of data that can be used to study
134 neighbourhood change, since any new datasets would need to be similarly processed in order to be
135 rendered compatible with these sources.

136 Another option considers the use of grid data (Dmowska et al., 2017; Dmowska and Stepin-
137 ski, 2018; Stepinski and Dmowska, 2019). Beyond the potentially increased spatial precision, this
138 approach does not require complex harmonisation when new data is considered, if the grids are
139 compatible. However, demographic data is usually not available in this format, especially from older
140 sources. Additionally, the conversion from tabulation areas can introduce significant errors.

141 Given these challenges, it is worth considering new alternatives. In this work, we propose a
142 novel methodology that entirely avoids the problems of geographical harmonisation, considering
143 each measurement using its actual geographic region. It does not require regions to be consistent
144 across time because they are naturally represented as different entities.

145 3.2 Data representation

146 Network based representation of geographic information is fairly well explored in the literature,
147 as a basis for topological methods for event detection (Doraiswamy et al., 2014), leveraging signal
148 processing on graphs (Shuman et al., 2013; Sandryhaila and Moura, 2013) to find patterns and
149 outliers (Valdivia et al., 2015; Dias and Nonato, 2015; Dal Col et al., 2018). Networks are well
150 suited to represent trajectories as well (Von Landesberger et al., 2016; Huang et al., 2016; Chen
151 et al., 2015), allowing the use of graph visualisation methods (Vehlow et al., 2015; Beck et al., 2014).
152 Our proposed method builds upon this literature. We leverage a network-based representation
153 that removes the requirement for consistency in the measurement regions. Each region in time
154 corresponds to a different node. Instead of a collection of time-series, the data is represented as a
155 dynamic network.

156 Networks have been used to represent census data for clustering purposes (Dias and Nonato,
157 2015; Setiadi et al., 2017), but these works did not explore temporal evolution, where they are
158 particularly powerful. Networks allow a natural representation of these inconsistent regions, with
159 both spatial and temporal connections. There are other possible representations that have similar
160 properties, but we adopted networks to allow the use of the vast existing literature and methods.

3.3 Data clustering and regionalisation

Data clustering is one of the elementary processes for data analysis, simplifying the data into a smaller number of homogeneous sets that can be interpreted in the same way. There is no shortage of contributions for this problem (Fahad et al., 2014), since variations of it appear in almost all scientific fields. Most neighbourhood related applications still rely on k-means (Jain, 2010; Delmelle, 2016), the Louvain method for community detection (Blondel et al., 2008; Thomas et al., 2012), or, to a lesser extent, Self Organising Maps (Delmelle, 2017; Ling and Delmelle, 2016; Arribas-Bel and Schmidt, 2013).

In geography, this problem is known as *regionalisation* (Montello, 2003), a rather old problem that has been thoroughly explored, leveraging different mathematical tools, including discrete topology (Brantingham and Brantingham, 1978) and discrete geometry (Assunção et al., 2006). Indeed, network-based methods are among the current state-of-the-art (Guo, 2008; Duque et al., 2012). However, *temporal* regionalisation is significantly less explored, especially in a demographic context, arguably due to the difficulties in dealing with unharmonised longitudinal data.

Since we adopted a network-based data representation and our objectives include an interactive interface, we opted for an heuristic variation of the maximum weighted matching algorithm called *sorted maximal matching* (Dias et al., 2017), because of its simplicity, customisability, and fast computation times. This algorithm merges clusters based on the weights of the edges between pairs of clusters, creating an hierarchy over the data, allowing the user to change the number of clusters without reprocessing the data. Changing the clustering algorithm would lead to different results, but any hierarchical network clustering method can be used in our framework. Indeed, our core contribution is a different interpretation of the data representation, not a new clustering or regionalisation method.

3.4 Cluster characterisation

While visualisation has gained prominence as a crucial component of scientific discovery, justification, and communication Tufte et al. (1998), visually representing evolving spatial data is a challenging old problem (Monmonier, 1990; Andrienko et al., 2003; Ferreira, 2015; Zheng et al., 2016).

Most geographic data is naturally bidimensional and maps work well in this case (Zheng et al., 2016; Ward et al., 2015), but the additional temporal dimension cannot be so naturally represented.

One straightforward option is to leverage tridimensional plots (Andrienko et al., 2014; Tominski and Schulz, 2012), but this can lead to visual obstructions or scaling problems unless a tridimensional display device is used. A simpler, well adopted, option is to display a map that corresponds to a subset of the temporal information, allowing the user to change the time with an associated control (Chen et al., 2017; Valdivia et al., 2015; Dal Col et al., 2018; Doraiswamy et al., 2014). Small multiples can be used (Von Landesberger et al., 2016), but only when there are few temporal snapshots. However, none of these options is suitable to represent many variables at the same time.

Using data clustering, we can represent the region’s cluster instead of all the its variables (Dal Col et al., 2018; Valdivia et al., 2015; Von Landesberger et al., 2016). While this simplifies the geographic portion of the visualisation, it introduces the problem of how to summarise the contents of each cluster. One traditional approach is to use parallel coordinates plot (Ferreira et al., 2015), but these they can get cluttered representing similar clusters over several variables. Further, for demographic applications, the clusters are usually strongly characterised by a small subset of values (Delmelle, 2016, 2017). Therefore, in the proposed method, we identify the variables that are most relevant to the characterisation of each cluster. The distribution of values on that variable is then represented using a boxplot, a well known statistical plot displaying basic properties of the distributions.

4 Visualising the demographic spatio-temporal evolution

Figure 2 presents an overview of the processing steps of the proposed method, illustrating how the nodes of the network are used to represent the regions. The following sections elaborate this figure and explain the main features of the interface we built to visualise and explore the evolution of neighbourhoods on the basis of our proposed method.

4.1 Census methodology and data representation

Census data is disseminated in a tabulated form for aggregation areas: whole country, state/province, metropolitan region, and so on. To allow for a more meaningful comparison of the data, we aggregated related variables (e.g. White, Black, Asian, Other) into what we called an *aspect* (e.g. Race). The aspects are represented using normalised histograms. This normalisation is crucial for direct comparison. In essence, it is a generalisation of the standard method of comparing percentages, since each aggregation area has a different total population.

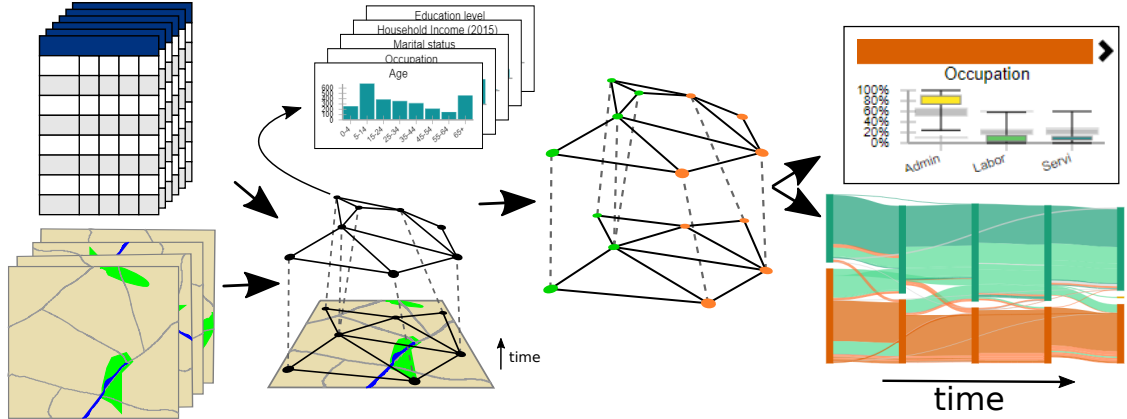


Figure 2: Overview of the proposed method. A network is generated combining the original census data, encoding the changing geographical information. The network is partitioned into an hierarchy (Dias et al., 2017). The characteristics and evolution of the clusters are then visually represented.

Each area of each census year is represented as a node, and edges are placed between nodes if the corresponding regions share geographic borders in the same year. Further, edges are placed between nodes if the corresponding regions belong to sequential years and their geometries intersect. To avoid spurious connections caused by geometry fluctuations, one of the geometries is slightly shrunk before the intersection, using a buffer of $-1e6$. More importantly, while weights will be associated with these edges before they are processed, they are not derived from the geometry, but from the data. The actual intersection area is not considered in this representation. This approach leads to a single network representing the whole spatio-temporal space of the data. Our objective then becomes to identify partitions of this network such that the nodes of each partition are more similar between themselves than to the other nodes.

4.2 Geographic content clustering

Having tied the regions together into a network, we can now partition it to identify similar sets of regions. We start by adopting a distance function between the nodes, measuring the difference between the data of the regions. This value is then associated with the edges, leading to a weighted dynamic network. Every node has a collection of histograms, each representing the distribution of certain aspect in the population.

Let $G = (V, E)$ be a network, where $V = \{v_1, v_2, \dots, v_n\}$ is the set of nodes and $E = \{(v_i, v_j), i \neq j \text{ and } i, j \in [1, n]\}$ is the set of edges. A function H associates each node to a set of K histograms.

236 We define the distance D between two nodes v_i and v_j as:

$$D(v_i, v_j) = \sum_{k \in [1, K]} w_k d(H_k(v_i), H_k(v_j)) \quad (1)$$

237 where d is a distance metric between histograms and w is a sequence of non-negative weights asso-
 238 ciated with each aspect, $\sum_{k \in [1, K]} w_k = 1$. While any histogram metric can be used, we adopted a
 239 euclidean distance between the vectors, because it led to reasonable results with reduced computa-
 240 tional cost. Therefore the distance between two nodes is defined as the weighted average distance
 241 between its associated histograms, where the weights can be adjusted by the user.

242 Once the distances are associated to the edges, we use watershed cuts (Cousty et al., 2009) to
 243 create an initial clustering, which is then refined into a hierarchy using the Sorted Maximal Matching
 244 (SMM) (Dias et al., 2017) with median linkage. The initial watershed step is performed to create
 245 an initial clustering and reduce the running time of the SMM. We introduced one new parameter to
 246 this method: a maximum distance threshold for the merges, to avoid the early merging of outliers.
 247 We refer the reader to the original paper (Dias et al., 2017) for more details, including a complete
 248 performance evaluation using several metrics. We chose this algorithm because it is simple and easily —
 249 customisable, and while different algorithms will lead to different results, our methodology should
 250 work with any hierarchical clustering algorithm.

251 Each resulting cluster is contiguous in the network. This means that two similar, but non-
 252 contiguous, sets of areas will be classified into two different clusters, which can be counter-intuitive.
 253 To overcome this issue, we *augment* the network with two new edges per node from a nearest
 254 neighbours graph (Pedregosa et al., 2011) using only the distances between the histograms. These
 255 edges connect nodes with similar content, if they are not already connected, providing a path for the
 256 algorithm to group similar nodes. The regions connected by those edges will be merged on the first —
 257 stages of the clustering, since they are very similar, leaving the remaining steps of the hierarchy to
 258 be determined only by the geographical edges. We explored with different numbers of augmentation
 259 edges, but the results were not consistent, since the distribution of the edges is data dependent.
 260 Adding two edges per node was the least number of edges that led to stable and consistent results
 261 in the scenarios available in our prototype. Since the problem of balancing the data space with the
 262 geographical space is relevant for geographical data analysis, this methodology potentially warrants
 263 further exploration, beyond the scope of this work.

4.3 Cluster characterisation and variable relevance

A crucial step in understanding neighbourhood change is to characterise the evolving clusters. The composition of each cluster is represented here by simple statistical measures, considering each aspect separately. We compute the minimum, maximum, median, 25%, and 75% quantiles for each variable of each aspect for all clusters in the hierarchy. While interpreting these values is more complex than interpreting just the average, they provide far more information about the underlying distribution.

We also use these statistical measurements to discover what characterises each cluster, that is, what makes it different from the others. We define the *relevance* of a variable of an aspect based on the distance between the interquartile ranges (IQR) of the clusters in the same hierarchical level. If the IQRs overlap for all clusters, that variable is not relevant to the characterisation of the cluster, but if the IQRs are distant, it means that this specific range of values is something that only occurs in this cluster. Examining IQRs therefore provides users a straightforward visual method for determining what variables most clearly define a given cluster.

4.4 Clusters and trajectories

While the partition of the data into different clusters helps the user to understand what groups exist and where they are, we are also interested in the evolution of these groups. To examine this process of evolution directly, we introduce the concepts of *temporal paths* and *trajectories*.

We call a temporal path any sequence of nodes in our representation network such that the temporal information associated with the nodes only increases. For instance, in Figure 1, the sequences ACF, ADF, ADG, and BEH are temporal paths. With harmonised data, the time-series of to each region would form a temporal path, each node would be connected only to its older and newer versions, belonging to only one temporal path, as illustrated by the path BEF. Since our data is not harmonised, more connections are allowed and each node can belong to an arbitrary number of paths.

Semantically, this is a generalisation of the idea of geographical time-series, because each temporal path is one possible option for the data to change over time. Returning to Figure 1, the paths ACF, ADF, and ADG all start on the same homogeneous region, but evolve differently over time. In other words, this network encodes the information that portions of the region A changed to form regions C and D, but we do not know specifically which parts, nor we need to, since the same region can

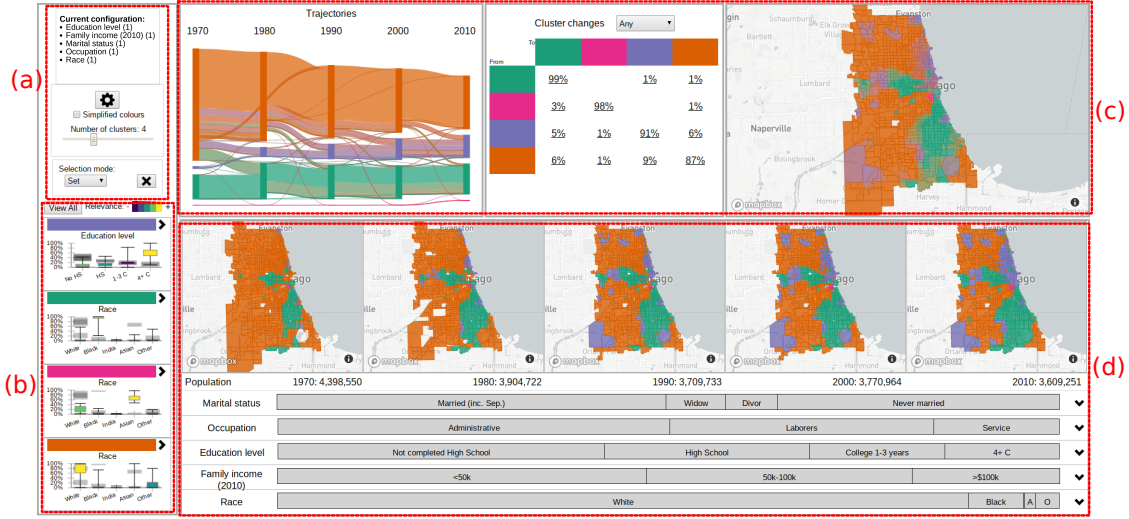


Figure 3: Initial interface of our method showing the demographic evolution of Chicago. **(a)**: Configuration panel with the current clustering parameters and controls. **(b)**: Cluster overview illustrating the most relevant aspect for each cluster. **(c)**: Trajectories overview and the general evolution of the population, geographical information, and how it changed. **(d)**: Details of the selected trajectories, including precise geographic locations, population numbers, and the composition of the aspects.

belong to several temporal paths. Interestingly, when interpreted in this framework, geographical harmonisation is a method to split and/or merge nodes so each belongs to a single temporal path.

Since each node in the sequence that forms the temporal paths has an associated cluster, we can classify the paths based on the sequence of clusters. We call each unique sequence of clusters present in this result a *trajectory*. Regions on the same trajectory had the same sequence of clusters, therefore had similar temporal evolution.

4.5 User interface

To validate and explore the results of our methodology, we built a user interface, illustrated in Figure 3, considering census tract (CT) level data from the Chicago region between 1970 and 2010. This region is known for its entrenched racial divide and the emergence of a ‘young urban’ population with a higher education level (Delmelle, 2016, 2017). More details are presented in Section 5.

As illustrated by Figure 3, our proposed interface heavily relies on colour to express cluster-related information. We adopted this convention because colours can be used in all our visual tools in a coherent manner. However, there is a limit on the number of distinct colours that can be used. We limited the number of clusters to eight because this was the largest number of colours that we

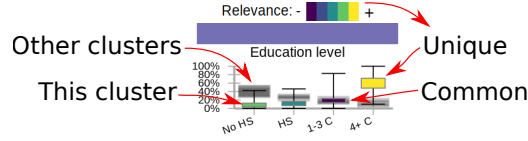


Figure 4: Enhanced boxplot of the clusters' characteristics allows a quick comparison to the other clusters.

could reliably and accessibly use, derived from the 8-class Dark2 set from ColorBrewer (Harrower and Brewer, 2003).

The configuration panel, on top left in Figure 3, displays which aspects were used and their weights (following Equation 1). It also includes other configuration options that can be altered without re-processing the data, such as the number of clusters and the colour option. The gear button allows access to the other configuration options that do require further processing, such as changing location, aspects, and weights.

The cluster overview panel, on the bottom left in Figure 3, displays a brief summary of each cluster, based on the distance between the IQRs, as detailed in Section 4.3. The *View all* button opens a new panel where all aspects are included, while the chevron at the side lets the user expand each cluster separately.

We adopted an *enhanced* version of the traditional boxplot, which includes the IQRs for the other clusters, in slightly larger and faded black rectangles. We also colour the current IQR according to its relevance. For instance, the boxplot that summarises the purple cluster illustrated in Figure 3, detailed on Figure 4, illustrates that this cluster is best defined by the proportion of the population with four or more years of college. The user can quickly see that this is relevant because the corresponding IQR is coloured with the highest relevance present in the legend. It is also clear that, while this cluster includes CTs that have between 10% to 90% of people in this variable, approximately, half of them have about 60% of the population with four or more years of college. Since all the other IQRs are well separated, this is a defining characteristic of this cluster. Conversely, the proportion of the population with one to three years of college is not relevant, as indicated by black fill in the rectangle representing the IQR of this cluster, in overlapping position with the rectangles of the other clusters. By clicking on the coloured bar above the boxplot, the user can select all trajectories that contain this cluster at any point in time.

The trajectories overview aims to convey basic information about the trajectories, where they are,

333 and what changes are involved. This is done using three sub panels. The first, on the left, contains
334 a Sankey diagram illustrating the evolution of the clusters over time. The widths are proportional
335 to the population involved. In our example in Figure 3, the orange and green clusters contain most
336 of the population and are fairly stable over time. The pink cluster is small and mostly stable. The
337 purple cluster is increasing, mostly by incorporating areas that were previously orange. Since the
338 purple group corresponds to the emergent 'young urban' group, this corroborates the findings of
339 Delmelle (Delmelle, 2016, 2017), showing that our network-based method can recover results from
340 the traditional data processing approach.

341 In the next panel, illustrated in the top middle of Figure 3, is a transition matrix between the
342 clusters. It indicates a rounded percentage of the population whose area changed between each pair
343 of clusters. This kind of table can be found in the related literature (Delmelle, 2016), so it is familiar
344 to the advanced users. It not only informs the proportional changes, but allows the selection of the
345 corresponding trajectories for further analysis.

346 The panel in the top right of Figure 3 is a map of the region under analysis, summarising the
347 geographical evolution of the clusters over time. The colours are derived from the clusters involved
348 in each trajectory, which are consistent across the linked views.

349 The bottom part of the interface contains the details for the selected trajectories, or for the whole
350 city if nothing is selected, as illustrated in Figure 3. This panel contains two main regions: the small
351 multiple maps, depicting the clusters at each year, and the stacked bar plots that summarise the
352 overall composition of these regions. In this example, the maps show the transition from orange to
353 green and purple in several regions over time. Clicking on a region in these maps will bring up a
354 new panel with the original census data of this specific region. The actual population numbers are
355 below the maps.

356 Each aspect is represented by a stacked bar plot, where the width of each rectangle corresponds
357 to the average percentage of that variable over the considered period. In this case, about half of the
358 people in this region, in the considered period, are married, and the percentage that are Widowers
359 or Divorced is roughly similar. About half of the population work in Administrative jobs, a third
360 never completed high-school, approximately half have gross family income below 50,000USD per
361 year. The vast majority identify as white. Placing the mouse over one of the bars will open a small
362 panel with the temporal evolution of that specific variable, and clicking on the chevron on the right
363 side expands the corresponding aspect, showing details of the temporal evolution of each variable

and also the corresponding IQRs for the whole city.

5 Illustrative scenarios

In this section we present two illustrative scenarios, using decennial census data from the United States (Manson et al., 2017) and Canada², tabulated by CTs, from 1970 to 2010. *Accidentally, the US data for 2010 is actually not from the decennial census, but from the ACS 2006-2010. Further, the regions selected do not correspond to any pre-defined regions (metros, cities, census areas), but to arbitrary regions defined around a location of interest. We selected a minimal set of aspects for each country, and they are not similar to each other, out of convenience, since the variable matching was a manual process. These caveats would likely compromise any serious attempt on a comprehensive demographic study, but this is not the objective of this experiment. We aim only to test and validate our methodology, comparing our results to pre-existing literature insights. Indeed, our results were perfectly aligned to several other studies, despite these methodological missteps, which could arguably be an indicator of the robustness of our method.*

The prototype interface allows access to 41 regions, 29 in the US and 12 in Canada. New York City was split into its boroughs to avoid memory crashes on the client browser due to the high number of CTs. We used five aspects for the USA: Education level, Family income, Marital status, Occupation, and Race; and seven for Canada: Age, Education level, Home language, Household Income, Marital status, Occupation, Place of birth, and Religion.

While our method does not require geographic harmonisation, it requires matching the variables over time. The supplementary material contains the details of which census columns were used for each aspect. Income is slightly inaccurate, even though we did correct for the official inflation. We grouped the original ranges into three larger ranges, but they do not match precisely.

These results are meant to demonstrate the utility of the interface for understanding the evolutionary dynamics of urban neighbourhoods. They also show the face validity of the results generated by our novel network-based approach.

²<http://datacentre.chass.utoronto.ca/census/>

5.1 Chicago

Our first scenario examines Chicago, focusing on a region loosely following the City’s administrative borders. Its demographic composition is well explored in the literature, with reports of racial divide and gentrification (Delmelle, 2016, 2017; Hwang and Sampson, 2014), so we expect our results to contain stable regions where the Race aspect is relevant, and some degree of population change, with increasing income and education levels.

The initial state of the prototype is illustrated in Figure 3. The first step is to identify the compositions of each cluster from the boxplots, so orange is associated with majority of White population, green with majority Black, and purple with higher proportion of four years of college or more (high education level). The expanded version of the boxplots for the purple cluster shows a higher income level and majority of occupations in administrative jobs, therefore the purple cluster identifies gentrified regions.

The trajectories plot illustrates the process of gentrification, also illustrated in Figure 5, progressively absorbing regions from the orange cluster (White). This corroborates results from the literature reporting that Black neighbourhoods are less likely to gentrify (Hwang and Sampson, 2014). Moreover, this process appears to be unidirectional, as indicated by the limited number of trajectories leaving the purple stream. Next, we select the region that is gentrified in 2010, by clicking on the corresponding rectangle in the trajectories plot, updating the information on the maps and the details portion of the interface.

The corresponding regions are highlighted in the maps, where the spatial pattern is clear, corresponding exactly to previous findings in the literature based upon harmonisation (Hwang and Sampson, 2014). Further, we can also identify the regions that gentrified earlier on the small maps that depict the involved regions over time. Since the most relevant aspect is Education, specifically “Four or more years of college”, we can expand the details of this aspect, as illustrated in the rightmost portion of Figure 5, which is increasing for the whole city (grey band), but faster and to a higher level in this region (black band).

5.2 Toronto

We consider a region that is approximately the administrative border of the current city of Toronto, using all seven available aspects with equal weights. While Chicago was fairly stable, Toronto is

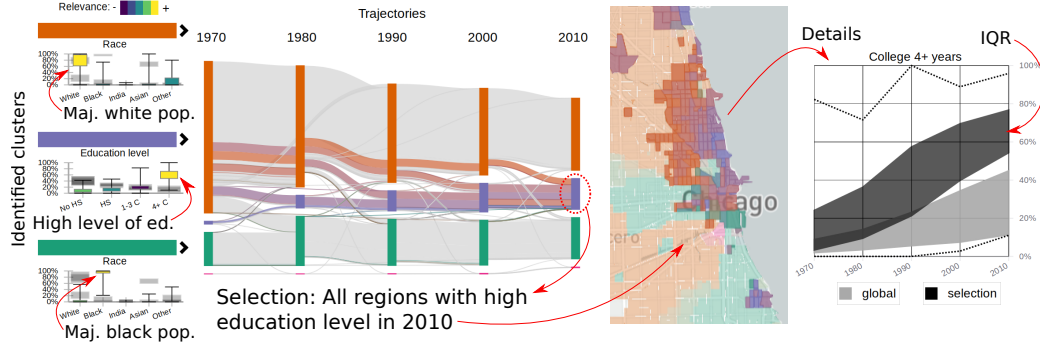


Figure 5: Workflow to discover gentrification in Chicago: the purple cluster corresponds to high education / income. Its population is increasing over time, absorbing from the majority White cluster (orange). By selecting the purple cluster in 2010, the region is highlighted in the maps. The proportion of people with 4+ years of college is increasing in the whole city (grey IQRs), but significantly more in this region (black).

known to be a more dynamic and diverse city, with significant and increasing immigrant popula- 418
tion (Hulchanski, 2007; Fong and Chan, 2011), especially Asian (Fong and Wilkes, 2003). Toronto is 419
also known for a stable and well defined Jewish community (Harold and Fong, 2018; Fong and Chan, 420
2011). Therefore, we expect a combination of stable and dynamic regions on the results, with Place 421
of Birth, Home Language, and Religion identified as relevant aspects. The results are summarised 422
in Figure 6, considering eight clusters. 423

The population with low percentage of University degrees is represented in orange, mostly an- 424
glophone population in green, Asian immigrants in yellow, high percentage of income in the highest 425
bracket in purple, high percentage of Jewish people in light green and brown, high percentage of 426
Eastern Non-Christian religion in pink, and high concentration of single people in dark grey. From 427
the trajectories plot, we can see that Toronto is more dynamic than Chicago, with one cluster con- 428
stantly shrinking. In the 1970s, the city was divided into four clusters: low number of university 429
degrees, Jewish population, majority anglophones, and high income. Interestingly, the more recent 430
clusters that absorbed regions from the orange cluster have similar education profiles and are differ- 431
entiated by other aspects. In this sense, the city is growing diverse, changing from a common low 432
education profile to a higher level of education with more diversity in religion (pink) and immigration 433
(yellow). 434

Indeed, the growing Asian population is visible starting in the 1980s and building thereafter, 435
leading to the yellow and pink clusters. While both include a high percentage of people born in 436
Asia, the pink is more defined by religion, with low percentage of university degrees, and contains the 437

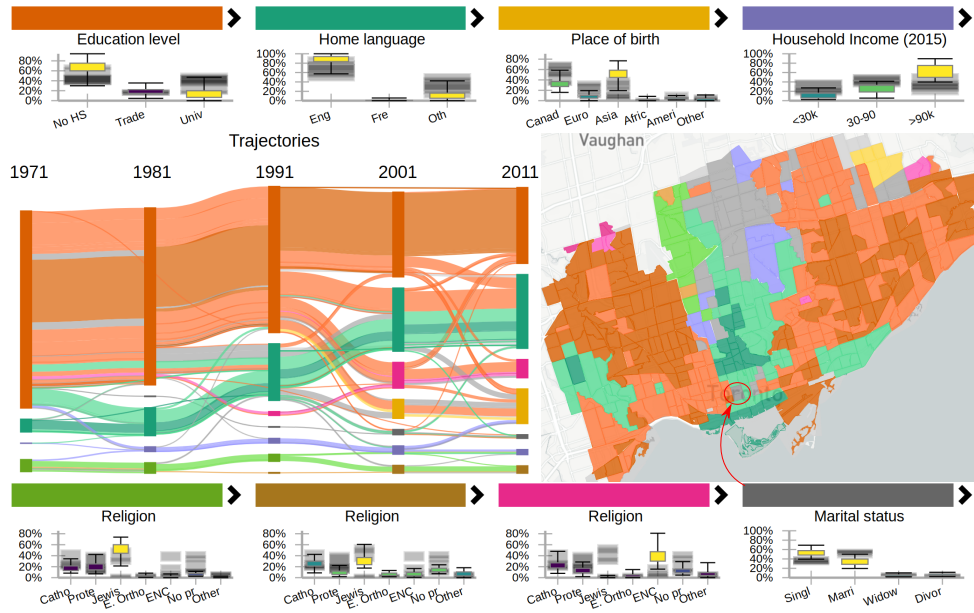


Figure 6: Clustering results for Toronto, with eight clusters, including clusters representing Jewish population, high and low income, low education, and Asian immigration.

lowest percentage of people in the highest income bracket for these clusters; the yellow is less defined by religion, and has higher education and income, geographically corresponding to the Markham region, known for its Chinese population. A similar division also happens for the two Jewish clusters, where the light green cluster has lower education and income levels than the brown cluster. The purple cluster of high income is somewhat stable. Until 2011 the cluster included the Bridle Path neighbourhood, known for its wealthy population. In 2011 it was classified into the yellow cluster of Asian immigration, since about 35% of the population for this CT were then born in Asia. The income distribution did not change, with 85% of the population with an income of 90k CAD or more.

The most significant indicator of Toronto's dynamism is the presence of grey regions on the map. These represent regions associated to three or more clusters over this five census period. Using the 'Add' mode for the trajectory selection, we select their trajectories, and a subset of the details is illustrated in Figure 7. These regions account for about 5% of Toronto's population. The whole region was classified into the orange cluster in 1971 (low level of university degrees). By 1991, most of the region was classified into the green cluster, representing anglophone population, mostly Canadian born, with a higher level of education. As the corresponding plot indicates, this trend in increasing education is city-wide, but this region has people with better education than most.

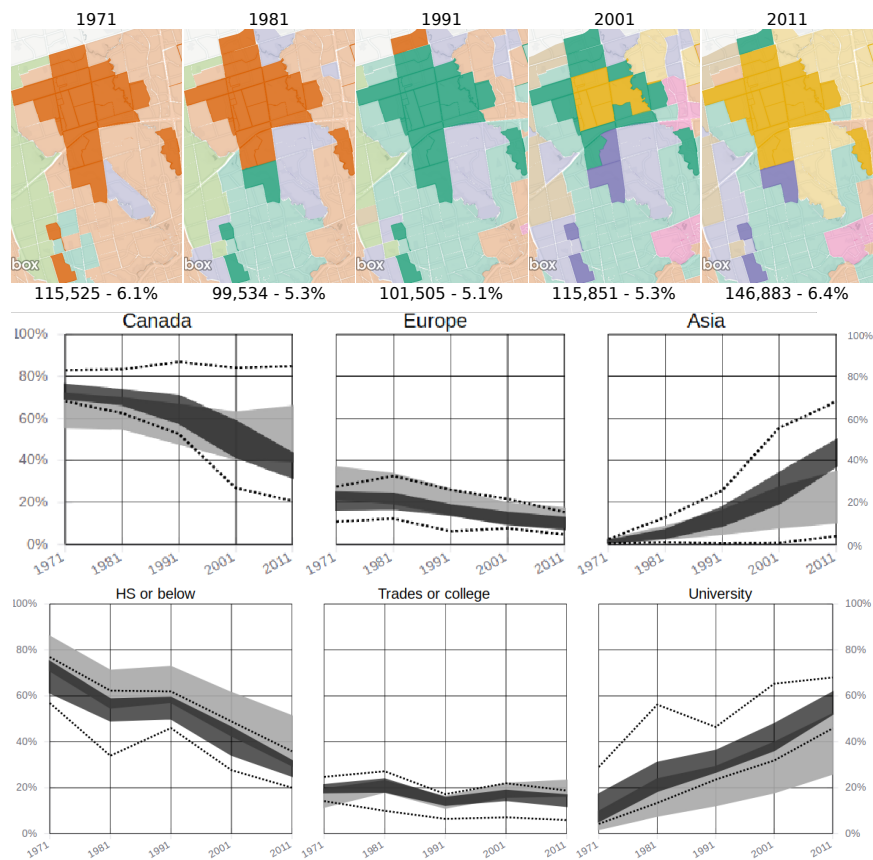


Figure 7: Details for some regions of Toronto that were classified into 3 or more clusters over time.

455 In 2001, the purple cluster of high income annexes neighbouring parts of the volatile region, and
456 the Asian born population increases sharply, as illustrated by the appearance of the yellow cluster.
457 This cluster indicates well educated, higher income, and about 30%-50% Asian born population. By
458 2011, the yellow cluster increased considerably, annexing parts of the high income purple cluster,
459 including the neighbouring Bridle Path area.

460 The geographical borders of the clusters obtained using our method are similar to the regions
461 presented by previous studies considering Toronto (Hulchanski, 2007). However, our interface pro-
462 vides a deeper insight into their demographic composition, since we consider more data than solely
463 Average Income, which appears to be a good proxy variable nonetheless. This scenario showcases
464 the ability of our method and interface to capture and understand the sources of urban volatility.

465 6 Expert feedback

466 As our method and tool are novel to the field, and somewhat exotic, we subjected them to the
467 critical scrutiny of experts. We contacted academic and industry experts in sociology and urban
468 sciences to solicit their evaluation of our methodology. They had access to the prototype tool, a
469 descriptive documentation of the features (included in the supplementary material), and a sequence
470 of documentation videos illustrating how to perform specific tasks. The documentation explains
471 which datasets are used and how the data is represented and processed, noting explicitly that there
472 is no geographic harmonisation. We focused our inquiries on the results obtained, asking if they
473 found anything interesting in the data. The message sent and their full response is included in the
474 supplementary material. Each of the five experts is identified by a letter, from A to E.

475 The overall overall response of the experts was positive, mentioning that the prototype allows
476 them to analyse census data without the additional work of obtaining and cleaning the data (A, B,
477 E), and it allows the inclusion of geographic visual analysis tools in their research process (D). It
478 enables the users to tell different stories about neighbourhoods/cities and their changes (A), visualise
479 the relationship between key urban variables over time (D), offering a quick way to identify particular
480 neighbourhoods that one may be interested in studying more in depth around a particular issue or
481 efficiently understanding the context of an area (E). Indeed, the experts identified gentrification
482 processes in Manhattan (B) and Dallas (E), reinforced a hypothesis for occupational clustering (D),
483 and highlighted how the method can be used to compare neighbourhoods and cities (A). In summary,

their view was that the proposed methodology can be a viable alternative for the visual analytics of evolving demographic data.

The interface was "easy to navigate" (B), but it was also considered "overwhelming" (A), "intimidating" (E), and "tricky to interpret" (C), possible side-effects of our effort to increase representational accuracy, where we avoided using simplified representation or labels. Identifying clusters by their most relevant variables was welcome, but the overlap of information from different clusters in the boxplot was "a bit confusing" (C) when colour was not present. Further, most clusters can be sufficiently characterised using only the most relevant aspect, but this is not generally true.

While the map of trajectories was mentioned as a "good summary map", how it related to the clustering method was unclear (C). The methods include different options on how the colours are used, but both are works in progress since reliably representing several distinct entities using colours is humanly unfeasible. Indeed, the number of distinguishable colours was a significant constraint, we found indications that more clusters should be used in some cases, even if eight clusters is more than what is traditionally considered in these analyses. Conversely, increasing the number of clusters would also complicate the interpretation of the results.

The experts also mentioned the poor responsiveness of the method when changes in the clustering parameters required server-side processing (B,D). Indeed, the current implementation can take a few minutes to cluster regions with high number of CTs, like Los Angeles or Brooklyn. Server-processing reduced the amount of data transferred to client, but it might increase the response time under load. We implemented a cache policy that greatly improved the performance, but fully pre-processing the results is not practical due to size of the parameter space.

Most of the experts demonstrated interest in using our method in their research (A, B, D, E), aiming to use the census data as a backdrop for other datasets, providing demographic context. They also mentioned the need to export subsets of data, plots, and maps to be used in reports and publications (C, D, E). More importantly, while these experts were aware that our method does not perform geographic harmonisation, none of them mention it. We did not specifically ask if this difference led to unexpected results, but rather if they found interesting insights.

7 Discussion and limitations

Our objective was to leverage a network based data representation and visualisation methods for the exploration of geographically inconsistent region-based data. While we successfully replicated and corroborated results from the literature, this method still has significant limitations.

Removing the need for geographical harmonisation greatly reduces the amount of work necessary to explore demographic data, but the method still requires consistent variables across the years. Matching the variables can be trivial for some aspects (Age), but challenging for others (Income). The divulged income ranges vary over time and the actual values change due to inflation. Some variables were not considered in earlier censuses, such as Race in Canada, or Hispanic population in the USA, hampering its use when they are available. Since this is only a prototype, we matched few aspects, but a proper demographic analysis would benefit from all available information.

The limitation on the number of displayed clusters because of the limited number of distinguishable colours was significant. While increasing the number of clusters would further complicate an already complex analysis, it might be warranted for some regions. Colour is a fundamental and intuitive tool for information representation that can be coherently used across different plots, so we opted to use it, even if in a limited way. With eight colours, there was overlap between some clusters, the relevance gradient, and the colour combination.

The cognitive load on the user is significant, as we compromised simplicity for accuracy. While other works labelled the clusters, as 'young urban', 'struggling', and so on (Delmelle, 2016, 2017), we show the statistical characteristics of the clusters, which are harder to interpret, as the data may have subtle nuances that labels would otherwise hide. This also led to a crowded interface, mitigated somewhat the use of pop-up panels and collapsible sections. For some cities, especially if they are small and stable, the panels can appear redundant, but each provide a different way to interact with the information that can ease the exploration process for larger and dynamic cities.

8 Conclusion

The objective of this work was to demonstrate that [temporal regionalisation can be performed without geographical harmonisation](#). We proposed an alternative methodology that robustly considers the data in its original geography, without the creation of arbitrary artificial data points.

This methodology was then used to create a publicly accessible system, with an interactive and

intuitive interface, allowing a transparent evaluation and replication of our results. We used this
 interface to corroborate results from the literature and we hope that it will be used to corroborate
 future results as well.

The feedback from experts was positive and most of them were able to extract insight from
 the prototype while indicating interest in using it for their research efforts. Since our interface
 can be used by non-experts as well, we also contributed to scientific dissemination and stakeholder
 transparency in urban sciences.

More importantly, we introduced a new idea that, apparently, was never considered in the litera-
 ture. While significant resources have been invested to improve geographical harmonisation, rarely,
 if at all, has anybody doubted that it was really necessary in the first place. We proved that it is
 not necessary, at least for the vast majority of demographic studies, especially for neighbourhood
 effects and neighbourhood dynamics.

References

- Abbott, A. (1997, 06). Of Time and Space: The Contemporary Relevance of the Chicago School.
Social Forces 75(4), 1149–1182.
- Allen, J. and Z. Taylor (2018). A new tool for neighbourhood change research: The canadian longi-
 tudinal census tract database, 1971–2016. *The Canadian Geographer / Le Géographe canadien*.
- Andrienko, G., N. Andrienko, H. Schumann, and C. Tominski (2014). Visualization of trajectory
 attributes in space–time cube and trajectory wall. In *Cartography from Pole to Pole*, pp. 157–163.
 Springer.
- Andrienko, N., G. Andrienko, and P. Gatalsky (2003). Exploratory spatio-temporal visualization:
 an analytical review. *Journal of Visual Languages & Computing* 14(6), 503–541.
- Arribas-Bel, D. and C. R. Schmidt (2013). Self-organizing maps and the us urban spatial structure.
Environment and Planning B: Planning and Design 40(2), 362–371.
- Assunção, R. M., M. C. Neves, G. Câmara, and C. da Costa Freitas (2006). Efficient regionalization
 techniques for socio-economic geographical units using minimum spanning trees. *International
 Journal of Geographical Information Science* 20(7), 797–811.

567 Beck, F., M. Burch, S. Diehl, and D. Weiskopf (2014). The State of the Art in Visualizing Dynamic
568 Graphs. In R. Borgo, R. Maciejewski, and I. Viola (Eds.), *EuroVis - STARs*. The Eurographics
569 Association.

570 Blondel, V. D., J.-L. Guillaume, R. Lambiotte, and E. Lefebvre (2008). Fast unfolding of communities
571 in large networks. *Journal of statistical mechanics: theory and experiment 2008*(10), P10008.

572 Brantingham, P. L. and P. J. Brantingham (1978). A topological technique for regionalization.
573 *Environment and Behavior 10*(3), 335–353.

574 Chen, W., F. Guo, and F.-Y. Wang (2015). A survey of traffic data visualization. *IEEE Transactions*
575 *on Intelligent Transportation Systems 16*(6), 2970–2984.

576 Chen, W., Z. Huang, F. Wu, M. Zhu, H. Guan, and R. Maciejewski (2017). Vaud: A visual
577 analysis approach for exploring spatio-temporal urban data. *IEEE Transactions on Visualization*
578 *& Computer Graphics*.

579 Cousty, J., G. Bertrand, L. Najman, and M. Couprie (2009, Aug). Watershed cuts: Minimum
580 spanning forests and the drop of water principle. *IEEE Transactions on Pattern Analysis and*
581 *Machine Intelligence 31*(8), 1362–1374.

582 Dal Col, A., P. Valdivia, F. Petronetto, F. Dias, C. T. Silva, and L. G. Nonato (2018). Wavelet-
583 based visual analysis of dynamic networks. *IEEE Transactions on Visualization and Computer*
584 *Graphics PP*(99), 1–1.

585 Delmelle, E. C. (2016). Mapping the dna of urban neighborhoods: Clustering longitudinal se-
586 quences of neighborhood socioeconomic change. *Annals of the American Association of Geogra-*
587 *phers 106*(1), 36–56.

588 Delmelle, E. C. (2017). Differentiating pathways of neighborhood change in 50 u.s. metropolitan
589 areas. *Environment and Planning A: Economy and Space 49*(10), 2402–2424.

590 Dias, F. and L. G. Nonato (2015). Some operators from mathematical morphology for the visual
591 analysis of georeferenced data. In *Workshop on Visual Analytics, Information Visualization and*
592 *Scientific Visualization - SIBGRAPI*.

- Dias, M. D., M. R. Mansour, F. Dias, F. Petronetto, C. T. Silva, and L. G. Nonato (2017, Oct). A hierarchical network simplification via non-negative matrix factorization. In *2017 30th SIBGRAPI Conference on Graphics, Patterns and Images (SIBGRAPI)*, pp. 119–126.
- Diez-Roux, A. V., F. J. Nieto, C. Muntaner, H. A. Tyroler, G. W. Comstock, E. Shahar, L. S. Cooper, R. L. Watson, and M. Szklo (1997). Neighborhood environments and coronary heart disease: a multilevel analysis. *American journal of epidemiology* 146(1), 48–63.
- Dmowska, A. and T. F. Stepinski (2018). Spatial approach to analyzing dynamics of racial diversity in large u.s. cities: 1990–2000–2010. *Computers, Environment and Urban Systems* 68, 89 – 96.
- Dmowska, A., T. F. Stepinski, and P. Netzel (2017, 03). Comprehensive framework for visualizing and analyzing spatio-temporal dynamics of racial diversity in the entire united states. *PLOS ONE* 12(3), 1–20.
- Doraiswamy, H., N. Ferreira, T. Damoulas, J. Freire, and C. T. Silva (2014, Dec). Using topological analysis to support event-guided exploration in urban data. *IEEE Transactions on Visualization and Computer Graphics* 20(12), 2634–2643.
- Duque, J. C., L. Anselin, and S. J. Rey (2012). The max-p-regions problem*. *Journal of Regional Science* 52(3), 397–419.
- Eicher, C. L. and C. A. Brewer (2001). Dasymetric mapping and areal interpolation: Implementation and evaluation. *Cartography and Geographic Information Science* 28(2), 125–138.
- Fahad, A., N. Alshatri, Z. Tari, A. Alamri, I. Khalil, A. Y. Zomaya, S. Foufou, and A. Bouras (2014, sep). A survey of clustering algorithms for big data: Taxonomy and empirical analysis. *IEEE Transactions on Emerging Topics in Computing* 2(3), 267–279.
- Ferreira, N. (2015). *Visual analytics techniques for exploration of spatiotemporal data*. Ph. D. thesis, Polytechnic Institute of New York University.
- Ferreira, N., M. Lage, H. Doraiswamy, H. Vo, L. Wilson, H. Werner, M. Park, and C. Silva (2015). Urbane: A 3d framework to support data driven decision making in urban development. In *Visual Analytics Science and Technology (VAST), 2015 IEEE Conference on*, pp. 97–104. IEEE.
- Firebaugh, G. and C. R. Farrell (2016, Feb). Still large, but narrowing: The sizable decline in racial neighborhood inequality in metropolitan america, 1980–2010. *Demography* 53(1), 139–164.

621 Fong, E. and E. Chan (2011). Residential patterns among religious groups in canadian cities. *City*
622 *& Community* 10(4), 393–413.

623 Fong, E. and R. Wilkes (2003, Dec). Racial and ethnic residential patterns in canada. *Sociological*
624 *Forum* 18(4), 577–602.

625 Galster, G. C. (2019). *Making our neighborhoods, making our selves*. University of Chicago Press.

626 GeoLytics, I. et al. (2010). Census neighborhood change database 1970—2010 census tract data.

627 Gotway, C. A. and L. J. Young (2002). Combining incompatible spatial data. *Journal of the*
628 *American Statistical Association* 97(458), 632–648.

629 Guo, D. (2008). Regionalization with dynamically constrained agglomerative clustering and parti-
630 tioning (redcap). *International Journal of Geographical Information Science* 22(7), 801–823.

631 Hallisey, E., E. Tai, A. Berens, G. Wilt, L. Peipins, B. Lewis, S. Graham, B. Flanagan, and N. B.
632 Lunsford (2017, Aug). Transforming geographic scale: a comparison of combined population and
633 areal weighting to other interpolation methods. *International Journal of Health Geographics* 16(1),
634 29.

635 Harold, J. and E. Fong (2018). Mnemonic institutions and residential clustering: Jewish residential
636 patterns in toronto. *Canadian Review of Sociology/Revue canadienne de sociologie* 55(2), 257–277.

637 Harrower, M. and C. A. Brewer (2003). Colorbrewer.org: An online tool for selecting colour schemes
638 for maps. *The Cartographic Journal* 40(1), 27–37.

639 Huang, X., Y. Zhao, C. Ma, J. Yang, X. Ye, and C. Zhang (2016, Jan). Trajgraph: A graph-based
640 visual analytics approach to studying urban network centralities using taxi trajectory data. *IEEE*
641 *Transactions on Visualization and Computer Graphics* 22(1), 160–169.

642 Hulchanski, D. J. (2007). The three cities within toronto: Income polarization among toronto’s
643 neighbourhoods, 1970-2005.

644 Hwang, J. and R. J. Sampson (2014). Divergent pathways of gentrification: Racial inequality and the
645 social order of renewal in chicago neighborhoods. *American Sociological Review* 79(4), 726–751.

646 Jain, A. K. (2010). Data clustering: 50 years beyond k-means. *Pattern recognition letters* 31(8),
647 651–666.

- Kwan, M.-P. (2018). The limits of the neighborhood effect: Contextual uncertainties in geographic, environmental health, and social science research. *Annals of the American Association of Geographers* 108(6), 1482–1490.
- Lee, A. C.-D. and C. Rinner (2015). Visualizing urban social change with self-organizing maps: Toronto neighbourhoods, 1996–2006. *Habitat International* 45, 92–98.
- Li, Y. and Y. Xie (2018). A new urban typology model adapting data mining analytics to examine dominant trajectories of neighborhood change: A case of metro detroit. *Annals of the American Association of Geographers* 108(5), 1313–1337.
- Ling, C. and E. C. Delmelle (2016). Classifying multidimensional trajectories of neighbourhood change: a self-organizing map and k-means approach. *Annals of GIS* 22(3), 173–186.
- Liu, X., Y. Song, K. Wu, J. Wang, D. Li, and Y. Long (2015). Understanding urban china with open data. *Cities* 47, 53 – 61. Current Research on Cities (CRoC).
- Logan, J. R., B. J. Stults, and Z. Xu (2016). Validating population estimates for harmonized census tract data, 2000–2010. *Annals of the American Association of Geographers* 106(5), 1013–1029.
- Logan, J. R., Z. Xu, and B. J. Stults (2014). Interpolating us decennial census tract data from as early as 1970 to 2010: A longitudinal tract database. *The Professional Geographer* 66(3), 412–420.
- Looker, B. (2015). *A nation of neighborhoods: imagining cities, communities, and democracy in postwar America*. University of Chicago Press.
- Manson, S., J. Schroeder, D. V. Riper, and S. Ruggles (2017). Ipums national historical geographic information system: Version 12.0 [database].
- Monmonier, M. (1990). Strategies for the visualization of geographic time-series data. *Cartographica: The International Journal for Geographic Information and Geovisualization* 27(1), 30–45.
- Montello, D. R. (2003). Regions in geography: Process and content. *Foundations of geographic information science*, 173–189.
- Pedregosa, F., G. Varoquaux, A. Gramfort, V. Michel, B. Thirion, O. Grisel, M. Blondel, P. Prettenhofer, R. Weiss, V. Dubourg, J. Vanderplas, A. Passos, D. Cournapeau, M. Brucher, M. Perrot,

675 and E. Duchesnay (2011). Scikit-learn: Machine learning in Python. *Journal of Machine Learning*
676 *Research* 12, 2825–2830.

677 Poorthuis, A. (2018). How to draw a neighborhood? the potential of big data, regionalization,
678 and community detection for understanding the heterogeneous nature of urban neighborhoods.
679 *Geographical Analysis* 50(2), 182–203.

680 Reades, J., J. D. Souza, and P. Hubbard (2019). Understanding urban gentrification through machine
681 learning. *Urban Studies* 56(5), 922–942.

682 Rey, S., E. Knaap, S. Han, L. Wolf, and W. Kang (2018). Spatio-temporal analysis of socioeco-
683 nomic neighborhoods: The open source longitudinal neighborhood analysis package (oslnap). In
684 *Proceedings of the 17th Python in Science Conference (SciPy 2018)*, pp. 121–128.

685 Sampson, R. J. (2012). *Great American city: Chicago and the enduring neighborhood effect*. Uni-
686 versity of Chicago Press.

687 Sandryhaila, A. and J. M. Moura (2013). Discrete signal processing on graphs. *IEEE transactions*
688 *on signal processing* 61(7), 1644–1656.

689 Setiadi, T., A. Pranolo, M. Aziz, S. Mardiyanto, B. Hendrajaya, and Munir (2017, Oct). A model
690 of geographic information system using graph clustering methods. In *2017 3rd International*
691 *Conference on Science in Information Technology (ICSITech)*, pp. 727–731.

692 Shelton, T. and A. Poorthuis (2019). The nature of neighborhoods: Using big data to rethink the
693 geographies of atlanta’s neighborhood planning unit system. *Annals of the American Association*
694 *of Geographers* 0(0), 1–21.

695 Shuman, D. I., S. K. Narang, P. Frossard, A. Ortega, and P. Vandergheynst (2013). The emerging
696 field of signal processing on graphs: Extending high-dimensional data analysis to networks and
697 other irregular domains. *IEEE Signal Processing Magazine* 30(3), 83–98.

698 Stepinski, T. F. and A. Dmowska (2019). Imperfect melting pot—analysis of changes in diversity and
699 segregation of us urban census tracts in the period of 1990–2010. *Computers, Environment and*
700 *Urban Systems* 76, 101–109.

- Stone, C. N., R. P. Stoker, J. Betancur, S. E. Clarke, M. Dantico, M. Horak, K. Mossberger, 701
J. Musso, J. M. Sellers, E. Shiau, et al. (2015). *Urban neighborhoods in a new era: Revitalization* 702
politics in the postindustrial city. University of Chicago Press. 703
- Thomas, I., C. Cotteels, J. Jones, and D. Peeters (2012, March). Revisiting the extension of the 704
brussels urban agglomeration : new methods, new data ... new results ? *Belgeo* (1-2). 705
- Tominski, C. and H.-J. Schulz (2012). The Great Wall of Space-Time. In M. Goesele, T. Grosch, 706
H. Theisel, K. Toennies, and B. Preim (Eds.), *Vision, Modeling and Visualization*. The Euro- 707
graphics Association. 708
- Tufte, E. R., S. R. McKay, W. Christian, and J. R. Matey (1998). Visual explanations: images and 709
quantities, evidence and narrative. 710
- Valdivia, P., F. Dias, F. Petronetto, C. T. Silva, and L. G. Nonato (2015, Oct). Wavelet-based 711
visualization of time-varying data on graphs. In *2015 IEEE Conference on Visual Analytics* 712
Science and Technology (VAST), pp. 1–8. 713
- Vehlow, C., F. Beck, and D. Weiskopf (2015). The State of the Art in Visualizing Group Structures in 714
Graphs. In R. Borgo, F. Ganovelli, and I. Viola (Eds.), *Eurographics Conference on Visualization* 715
(EuroVis) - STARs. The Eurographics Association. 716
- Von Landesberger, T., F. Brodtkorb, P. Roskosch, N. Andrienko, G. Andrienko, and A. Kerren 717
(2016). Mobilitygraphs: Visual analysis of mass mobility dynamics via spatio-temporal graphs 718
and clustering. *IEEE transactions on visualization and computer graphics* 22(1), 11–20. 719
- Ward, M. O., G. Grinstein, and D. Keim (2015). *Interactive data visualization: foundations, tech-* 720
niques, and applications. AK Peters/CRC Press. 721
- Zheng, Y., W. Wu, Y. Chen, H. Qu, and L. M. Ni (2016, Sept). Visual analytics in urban computing: 722
An overview. *IEEE Transactions on Big Data* 2(3), 276–296. 723